

Interaction of Counterions with Subtilisin in Acetonitrile: Insights from Molecular Dynamics Simulations

Diana Lousa,[†] Michele Cianci,[‡] John R. Helliwell,[§] Peter J. Halling,^{||} António M. Baptista,[†] and Cláudio M. Soares*,[†]

[†]Instituto de Tecnologia Química e Biológica, Universidade Nova de Lisboa, Av. da República, 2780-157 Oeiras, Portugal

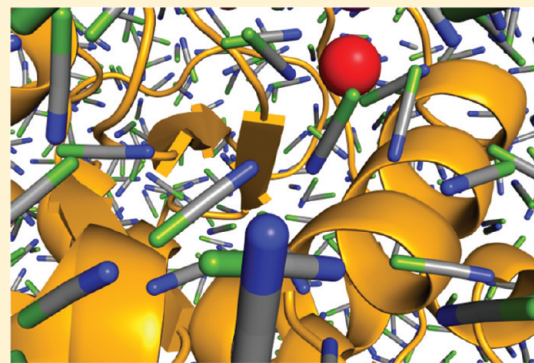
[‡]European Molecular Biology Laboratory, Hamburg Outstation, c/o DESY, Building 25a, Notkestraße 85, 22603 Hamburg, Germany

[§]Department of Chemistry, University of Manchester, Manchester M13 9PL, United Kingdom

^{||}WestCHEM, Department of Pure & Applied Chemistry, University of Strathclyde, Glasgow G1 1XL, United Kingdom

S Supporting Information

ABSTRACT: A recent X-ray structure has enabled the location of chloride and cesium ions on the surface of subtilisin Carlsberg in acetonitrile soaked crystals.¹ To complement the previous study and analyze the system in solution, molecular dynamics (MD) simulations, in acetonitrile, were performed using this structure. Additionally, Cl^- and Cs^+ ions were docked on the protein surface and this system was also simulated. Our results indicate that chloride ions tend to stay close to the protein, whereas cesium ions frequently migrate to the solvent. The distribution of the ions around the enzyme surface is not strongly biased by their initial locations. Replacing cesium by sodium ions showed that the distribution of the two cations is similar, indicating that Cs^+ can be used to find the binding sites of cations like Na^+ and K^+ , which, unlike Cs^+ , have physiological and biotechnological roles. The Na^+Cl^- is more stable than the Cs^+Cl^- ion pair, decreasing the probability of interaction between Cl^- and subtilisin. The comparison of water and acetonitrile simulations indicates that the solvent influences the distribution of the ions. This work provides an extensive theoretical analysis of the interaction between ions and the model enzyme subtilisin in a nonaqueous medium.



INTRODUCTION

Although most enzymes have evolved to catalyze reactions in an aqueous environment, the use of nonaqueous solvents as reaction media is not only feasible but can also be advantageous.² The biotechnological potential of nonaqueous biocatalysis has attracted the attention of researchers over the last three decades. These researchers have addressed and elucidated questions such as the structure, dynamics, and stability of enzymes in nonaqueous solvents,^{3–15} the role played by water,^{10,16–22} the influence of the solvent and reaction conditions (e.g., amount of water) on enzyme selectivity,^{17,23–26} and the interesting phenomena of pH memory^{27,28} and ligand imprinting.^{29–31}

Another issue that has gathered the attention of researchers in this field is the effect of ions and other compatible solutes on enzyme activity, stability, and enantioselectivity.^{32–35} Several studies have shown that lyophilizing the enzyme in the presence of salts enhances its catalytic activity in organic solvents.^{36–39} Moreover, it has been observed that the degree of activation depends on the nature of the salt and that the combination of a kosmotropic anion and a chaotropic cation usually gives the best results.⁴⁰ Despite the large number of studies in this area, the mechanism through which the ions stabilize and enhance the activity of enzymes remains elusive. In

some cases, it seems that the ions change the mobility of the water molecules that surround the protein.⁴¹

The interaction between the enzyme molecule and its counterions is strongly dependent on the properties of the solvent.⁴² In solvents with high dielectric constants, like water, the ions tend to be dispersed in solution and generally would not be expected to form stable interactions with the protein. In apolar solvents, on the other hand, the ions are expected to form very strong salt bridges with the charged groups of the protein, playing a very important role in stabilizing the enzyme. A more complex problem is to determine how the counterions interact with the enzyme when the reaction takes place in a moderately polar solvent like acetonitrile.

Subtilisin Carlsberg is a serine protease secreted by some strains of the Gram-positive bacterium *Bacillus subtilis*. Like all serine proteases, it has a catalytic triad, composed by a serine, a histidine, and an aspartate. It converts a large number of substrates and is able to perform both hydrolytic and esterification reactions, being more active under alkaline conditions, where the catalytic triad tends to have a global

Received: February 10, 2012

Revised: April 28, 2012

Published: April 30, 2012

Table 1. Overview of the MD Simulations Performed to Tackle the Main Questions of This Work

question	protonation state of Ne_2 of H64	solvent	cations	anions	method used to place ions	number of replicates	simulation time
1. Do the ions in solution occupy the same sites as in the X-ray structure?	protonated	acetonitrile	11 Cs^+	8 Cl^-	X-ray structure	20	10 ns
2. Are the simulations biased by the initial locations of the ions?	protonated	acetonitrile	4 Cs^+	6 Cl^-	docking-based methodology ^a	20	10 ns
3. How does the solvent influence the behavior of the ions?	protonated	water	11 Cs^+	8 Cl^-	X-ray structure	20	10 ns
4. What is the effect of replacing Cs^+ with Na^+ ?	protonated	acetonitrile	11 Na^+	8 Cl^-	X-ray structure (Cs^+ positions)	20	10 ns
5. What is the influence of the protonation state of H64?	deprotonated	acetonitrile	11 Cs^+/Na^+	8 Cl^-	X-ray structure	20	10 ns
6. How are ions distributed around the protein in water?	protonated	water	271 Cs^+	273 Cl^-	random ^b	5 ^c	50 ns ³

^aThis methodology is described in detail in the Supporting Information. ^bThe method that was used to randomly distribute the ions in these simulations is described in the Supporting Information. ^cTo make sure that the ions that were initially randomly distributed in solution (far from the protein) would have enough time to reach the protein surface and explore a large number of binding sites, and given that in water simulations the enzyme is stable, five replicates of 50 ns were used, amounting to a total of 250 ns, which enables a good sampling.

negative charge. Subtilisin Carlsberg is active in a large number of nonaqueous solvents and is often used as a model enzyme in nonaqueous enzymology. Several structures of this enzyme in the presence of organic solvents have been obtained^{1,43–45} (by soaking the cross-linked crystals with the solvent), and its catalytic behavior in nonaqueous media has been extensively studied (see, e.g., ref 2).

In a recent work, the X-ray structure of subtilisin Carlsberg soaked in acetonitrile and cesium chloride was obtained to determine the positions of chloride and cesium ions in the conditions found in the crystal environment.¹ This was important to the understanding of the interaction between enzymes and counterions in nonaqueous media. However, X-ray crystallography techniques generally give us a static perspective of reality, or certainly an average of many possible conformations in the crystal, and yet a dynamic picture is essential to gain a deeper knowledge of this problem. Additionally, the crystal environment, despite being similar to solution, is not exactly a free solution and crystal contacts can constrain the structure of the protein and influence the distribution of counterions. Herein, we complement the previous study by using a molecular dynamics (MD) simulation approach to characterize the interaction of counterions with subtilisin in acetonitrile solution and to obtain a dynamic perspective of this interaction.

MATERIALS AND METHODS

Calculation of the Potentials of Mean Force (PMFs).

Before analyzing the interaction of counterions with subtilisin, we wanted to know how chloride ions interact with cesium and sodium ions in solvents with different polarities. Toward this end, we calculated the potentials of mean force between the anion (Cl^-) and the cation (Cs^+ or Na^+) in three different solvents: water, acetonitrile, and hexane. The calculation of the potentials of mean force was done using a methodology based on constrained MD simulations.^{46,47} This methodology was implemented by performing MD simulations with the application of distance constraints between the cation and the anion at many different distance values. The mean force at each constrained distance is then given by the negative of the average constraint force, and the PMF is obtained by integrating the mean force over the ion separation distances.^{46,47}

To calculate the PMF between an ion pair in a given solvent, the cation and anion were placed in the center of a

dodecahedron box that was filled with the solvent of interest. The distance between ions was constrained to values between 0.2 and 1.2 nm in intervals of 0.02 nm, using the LINCS algorithm,⁴⁸ and for each distance, a MD simulation of 1 ns was performed. The MD simulations were performed as described below (see Setup for MD Simulations). Note that, contrary to previous implementations of the methodology,^{46,47} we used a reaction field correction to treat long-range electrostatic interactions.

MD Simulations. Although the recent determination of the X-ray structure of subtilisin Carlsberg in acetonitrile in the presence of CsCl has enabled the determination of the counterions' binding sites in the crystal conditions, several questions remain unanswered. In order to have a complete picture of the interaction between subtilisin and counterions in acetonitrile solution, we have performed an extensive study, comprising a large number of MD simulations in different conditions. In this study, we have addressed several questions and used different sets of MD simulations (which are summarized in Table 1) to tackle these questions.

Protein Structures Used in the MD Simulations. The crystallographic structure of subtilisin Carlsberg obtained by Cianci et al. at 2.24 Å resolution, after soaking the crystals with CsCl (PDB ID: 2WUV),¹ was used in the simulations where the ions were kept in their crystallographic binding sites. In the simulations where the ions were placed according to our docking methodology, we used the structure determined by the same authors at 2.23 Å resolution, in the absence of CsCl (PDB ID: 2WUW).¹ All water and acetonitrile molecules found in the X-ray structure were used in our simulations.

Modeling Protein Protonation Equilibrium. The determination of the pK_a of each titrable site in the protein was performed using a methodology developed by us, based on continuum electrostatics and Monte Carlo sampling of protonation states that has been explained in detail before^{49,50} (the details of the protocol that was used can be found in the Supporting Information).

Setup for MD Simulations. The methodology used in the molecular dynamics simulations is similar to the one that we have used in many previous studies and is explained in detail elsewhere.¹⁰ MD simulations were performed with the GROMACS package,⁵¹ version 4.0,⁵² using the GROMOS S3A6 force field.⁵³ Water was modeled with the simple point charge (SPC) model,⁵⁴ the parameters from Gee et al.⁵⁵ were

used for acetonitrile, and hexane was treated as a flexible united atom model using the GROMOS 53A6 parameters for alkanes.⁵³ The parameters of Reif et al.⁵⁶ were used for sodium, cesium, and chloride ions. Bond lengths of the solute, acetonitrile, and hexane molecules were constrained with LINCS,⁴⁸ and SETTLE⁵⁷ was used for water. The simulations were performed at constant temperature and pressure. Temperature coupling was implemented using the Berendsen thermostat⁵⁸ with a reference temperature of 300 K. For the simulations carried out in acetonitrile and hexane, the protein, ions, and water were coupled to the same heat bath and the solvent was coupled to a separate heat bath. For the aqueous simulations, the protein and ions were coupled to the same heat bath and water was coupled to a separate heat bath. The pressure control was done by applying the Berendsen algorithm⁵⁸ with an isotropic pressure coupling, using a reference pressure of 1 atm and a relaxation time of 0.5, 1.3, and 1.5 ps for water, acetonitrile, and hexane simulations, respectively. An isothermal compressibility of 4.5×10^{-5} bar⁻¹ was used for all the solvents. Nonbonded interactions were calculated using a twin-range method with short- and long-range cutoffs of 0.8 and 1.4 nm, respectively.⁵⁹ A reaction field correction for electrostatic interactions was applied,^{60,61} considering a dielectric constant of 54⁶² and 35.84⁶³ for water and acetonitrile, respectively. The preparation of the systems to run the production MD simulations can be found in the Supporting Information.

RESULTS AND DISCUSSION

Potentials of Mean Force between the Cations, Cs⁺ and Na⁺, and the Anion, Cl⁻, in Solvents with Different Polarities. Before studying the interaction between ions and subtilisin, we considered that it was relevant to analyze how the isolated cations, Cs⁺ and Na⁺, each separately interact with the anion, Cl⁻, in solvents with different polarities, namely, water, acetonitrile, and hexane. Toward this end, we calculated the potentials of mean force (PMFs) between the anion and the cation in these solvents (the results are shown and discussed in detail in the Supporting Information). Our results indicate that in hexane the interaction between oppositely charged ions is very strong and the ions form highly stable complexes that are never broken at room temperature (see Figure S2, available in the Supporting Information). In contrast, in water, the ions tend to be dispersed and do not form stable complexes at room temperature (as can be observed in the same figure). The PMF analysis displayed in Figure S2 (available in the Supporting Information) indicates that in acetonitrile the ions form stable associations, which was confirmed by unconstrained MD simulations (see Figure S3 in the Supporting Information). Our PMF analysis not only provides a description of how sodium and cesium interact with chloride in different media, but more generally, it gives us an idea of how oppositely charged particles interact in these media. On the basis of these results, one can expect the interaction between these ions and protein charged groups in acetonitrile to be stable.

Determination of the Protonation State of Ionizable Residues at pH 6.5. Before starting a MD simulation of a protein, one needs to determine the protonation states of all the ionizable residues at the pH of interest. The solution that was used to soak the subtilisin crystals had a pH of 6.5, and therefore, this was the pH value that was considered when assigning the protonation states. The determination of the pK_a values of all the titrable residues of subtilisin was performed

using a methodology based on continuum electrostatics, and the results are available in the Supporting Information. Our results indicate that, at the pH of interest (6.5), the protonated fraction of the catalytic histidine (H64) is around 70% (Figure S4 in the Supporting Information). This means that both states (fully protonated and partially deprotonated) are expected to coexist at this pH. Although, according to our calculations, the fully protonated state is the predominant one, it is believed that this residue must be partially deprotonated in order to accept the proton from serine 221 during the catalytic process. Therefore, both states were considered in our MD simulations.

Stability of the Simulations. The temporal evolution of the root-mean-square deviation (rmsd) from the X-ray structure and secondary structure content can be used to analyze the stability of a protein during a MD simulation. It is clear from Figure 1 and Figures S5 and S6 (available in the

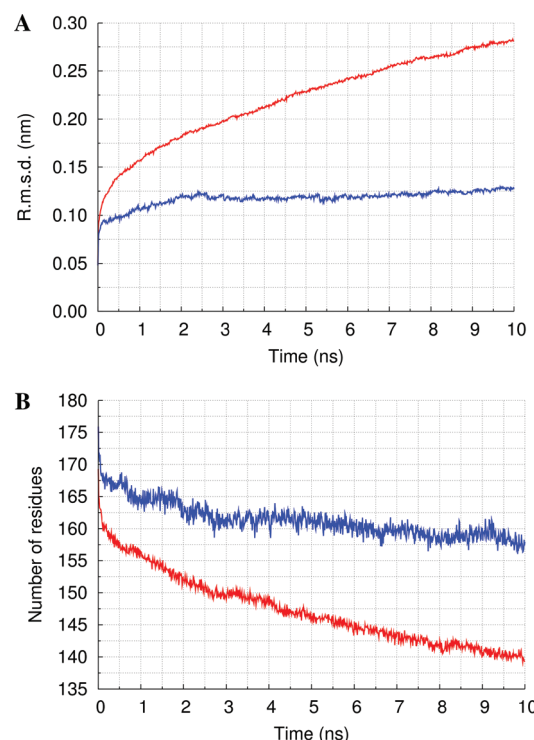


Figure 1. Temporal evolution of the average root-mean-square deviation (rmsd) of C α atoms from the X-ray structure (A) and the average secondary structure content (B). The averages were calculated using all the simulations performed in each solvent (80 and 25 for acetonitrile and water, respectively (see Table 1)). The secondary structure content was computed as the sum of the number of residues that are part of α -helices, β -sheets, β -bridges, or turns, according to the DSSP criterion.⁶⁴ The blue and red lines correspond to the simulations performed in water and acetonitrile, respectively.

Supporting Information) that subtilisin is much more unstable in acetonitrile than in water simulations. These results are in line with previous MD simulation studies which show that subtilisin undergoes large conformational changes in acetonitrile.¹¹ The fact that the X-ray structure obtained shows a fold in acetonitrile very similar to the one obtained in water is probably a consequence of the glutaraldehyde cross-linking performed before washing the crystals with acetonitrile. When enzymes are industrially used in acetonitrile, they will almost always be in some constrained solid state, immobilized on a surface, cross-linked, or even in crystals, all prepared initially in

aqueous media, and therefore, the X-ray structure provides a good model of the interaction of counterions with subtilisin in these conditions. Our results indicate that during the simulation a considerable fraction of intra-main-chain hydrogen bonds are replaced by hydrogen bonds with acetonitrile molecules (data not shown). This can, at least partially, account for the loss of secondary structure that is observed in the MD simulations.

The analysis described above indicates that it is risky to prolong the simulations in acetonitrile for more than 10 ns, because the protein structure starts to show signs of unfolding. Therefore, although it would be desirable to have longer simulations, we decided to stop them at 10 ns. At this point, the enzyme structure is still reasonably similar to the X-ray structure (see Figure S5 in the Supporting Information), which means that the ion distributions will not be affected by large protein conformational changes. Given that we cannot have longer simulations, to achieve more sampling, we used a large number of replicates (20) for each condition.

Comparison of X-ray and Docking Ion Binding Sites.

As was described above (see Table 1), we used two different strategies to find the initial locations of counterions. In the first approach, we used the previously determined X-ray structure with bound Cs^+ and Cl^- ions.¹ Additionally, we also placed ions using a docking protocol previously developed by us,¹⁰ which provides another reference to compare the ions' behavior in MD simulations using different initial positions. This unbiased protocol (which is described in the Supporting Information) docks ions on the enzyme surface until all the protein side chains are neutral. In Figure 2, the locations of counterions

was found to be the most attractive site for Cl^- ions by our docking methodology (a very positively charged region formed by the N-terminus and a calcium ion) did not contain any Cl^- ion in the X-ray structure.

The number of cesium positions found by our docking methodology (4) is considerably smaller than in the X-ray structure (11). However, the sum of the X-ray crystal structure derived occupancies of the Cs^+ ions is 2.90, which indicates that there are various sites with the capacity to bind Cs^+ , but only a fraction can be occupied around a given protein molecule, in part because of repulsion between the Cs^+ . In the crystals, different sites are occupied on different molecules, leading to the observed partial occupancy. Similarly to what was observed for chloride ions, three approximately coincident binding sites were found with the two approaches.

There are two constraints that account for the observed differences in the locations of the ions found by the two methodologies. The first one is the fact that contacts between adjacent molecules in the crystal can create artificial binding sites that are not found in solution. Indeed, in this specific case, there are a large number of ions coordinated by two or more distinct protein molecules in the X-ray crystal structure. The second reason that can explain the observed differences is the fact that, in our docking methodology, the positive and negative ions are docked separately, whereas, obviously, in the soaking solution both ions are present simultaneously. This explains why Cl^- and Cs^+ ions never form ion pairs in the docking methodology, contrary to what is observed in the X-ray crystal structure.

Occupancy of the Ion Binding Sites during MD Simulations.

In order to evaluate the affinity of chloride and cesium ions for the binding sites that were found in the X-ray structure or using our docking methodology, we calculated the occupancy of each of these binding sites throughout the last 8 ns of simulation. This occupancy corresponds to the fraction of time during which the binding site is occupied by a Cl^- or Cs^+ ion.

In Figure 3, ions are colored according to the occupancies of the original binding site. It is clear from Figure 3A that the affinity of Cl^- ions for the X-ray binding sites in acetonitrile simulations displays a high variability. Half of the binding sites have occupancies greater than 0.5, and the occupancies range from very low (there is one binding site with an occupancy less than 0.1) to high (one of the binding sites is occupied more than 80% of the time). In the simulations performed with the docked ions, five of the six chloride binding sites have an occupancy superior to 0.9 (see Figure 3C), indicating that these sites are very attractive locations for Cl^- ions. Cesium ions exhibit a very different behavior. As can be observed in Figure 3B and D, most Cs^+ ions have occupancies lower than 0.1. These cations do not spend much time in any of the binding sites, irrespective of whether these sites are the crystallographic ones or the ones obtained with our docking methodology.

One of our aims was to analyze the effect of replacing cesium by sodium ions. Comparing Figure 3B and F, we can see that there are two binding sites which are considerably more populated by Na^+ than by Cs^+ (blue and cyan spheres in Figure 3F). As can be found by comparing Figure 3A and E, replacing the cations influences the behavior of some of the Cl^- anions. Four of the chloride binding sites which had an occupancy superior to 0.6 in the presence of cesium (cyan and blue spheres in Figure 3A) are less populated when cesium is replaced by sodium. Visual analysis of the trajectories indicates

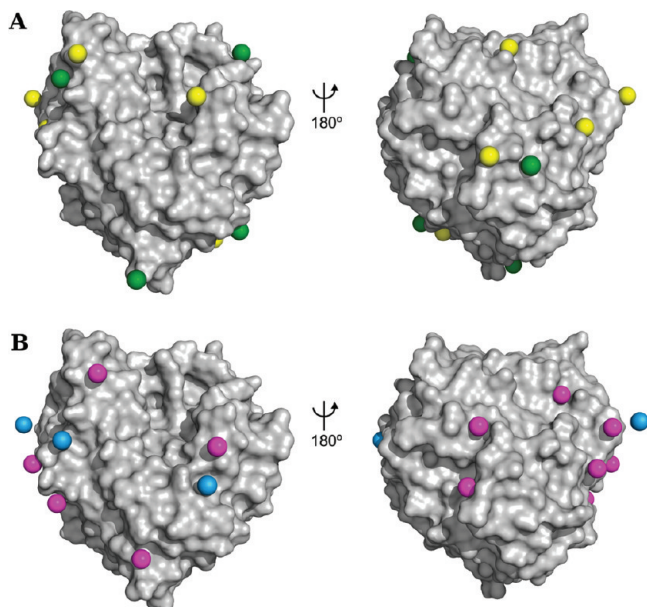


Figure 2. Comparison of X-ray and docking binding sites for (A) the chloride ions, yellow and green, respectively, and (B) the cesium ions, magenta and blue, respectively.

obtained in the X-ray structure and using our docking methodology are compared. In the upper part of the figure, the binding sites of chloride ions are shown. The occupancies of the eight crystallographic Cl^- sites sum to a total of 4.65 which is close to the number of docked chlorides (6). Three of the six Cl^- binding sites found with our docking methodology are close to crystallographic binding sites, although they are not interacting with the same residues. Intriguingly, the region that

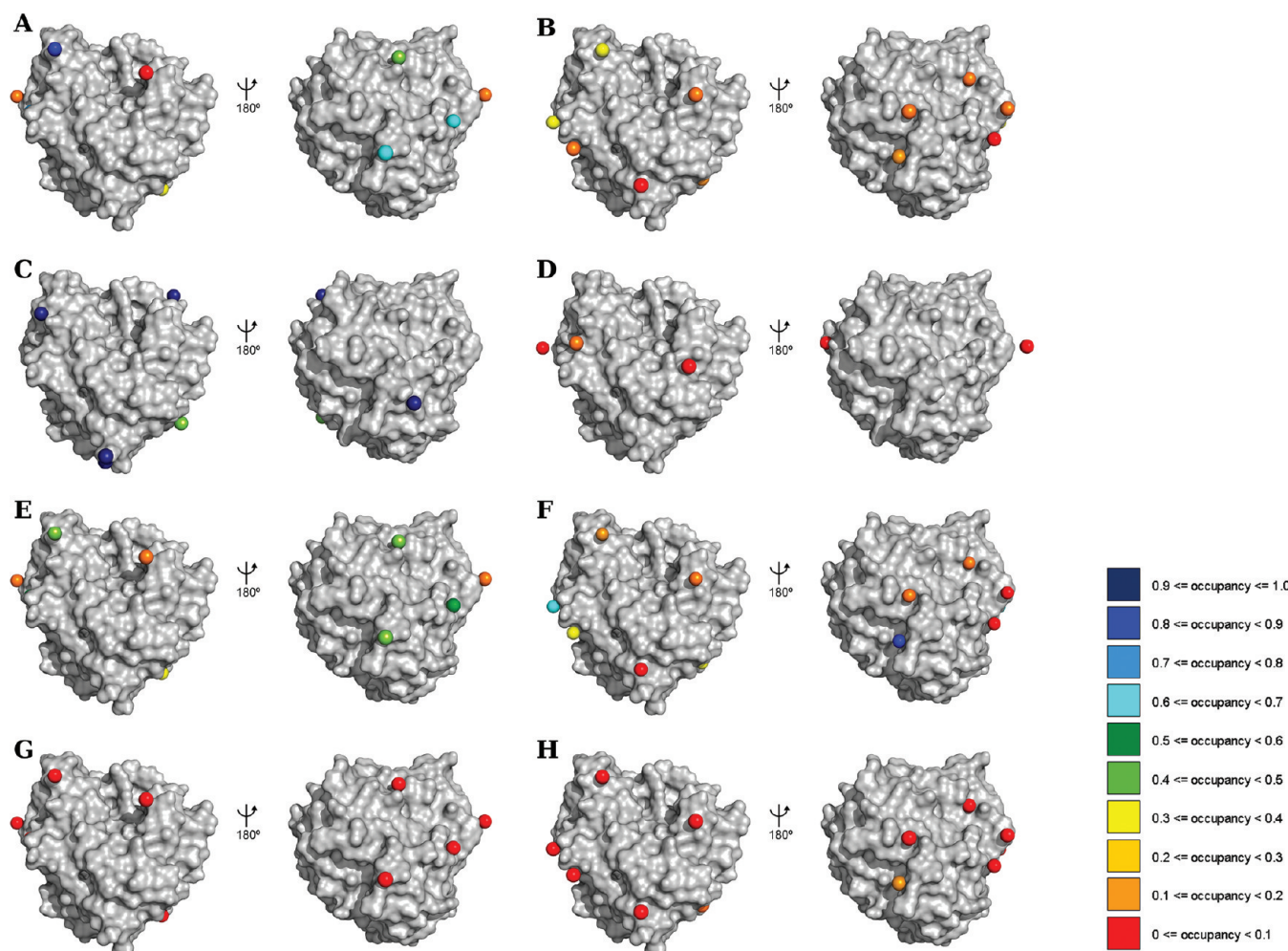


Figure 3. Occupancies of the original ion binding sites during MD simulations. The spheres represent the chloride (left side) and cesium or sodium ions (right side) placed in the initial binding sites and colored according to the respective occupancy (see scale). A and B correspond to the X-ray binding sites; C and D correspond to the locations found with the docking method; E and F correspond to the simulations where the X-ray cesium ions were replaced by sodium ions; and G and H correspond to the simulations in water using the X-ray positions. To calculate the occupancy, we first found the residues which comprise each binding site and then counted the number of frames in which the minimum distance between these residues and the corresponding ion was smaller than 0.4 nm (this cutoff was chosen after inspecting the histogram of the minimum distance between the ions and binding site residues) and then divided this value by the total number of frames.

that the chloride ions often form ion pairs with sodium ions and these ion pairs can (temporarily) migrate to the solvent. This behavior is not observed when the cation used is cesium, which makes sense in the light of our previous results that showed that the Na^+Cl^- ion pair is stronger than its Cs^+Cl^- counterpart (see the potential of mean force analysis, above).

In order to elucidate the role played by the solvent in the observations described above, we performed control MD simulations in water. Figure 3G and H shows that, in these simulations, both Cl^- and Cs^+ have low occupancies (in most cases, lower than 0.1). This is not surprising, if we think that, in aqueous media, ions are generally found in the bulk solution rather than on the enzyme surface (except in the case of high affinity binding sites). This is also consistent with our potential of mean force PMF analysis (see above) that shows that cesium and chloride tend to be dissolved in water.

Distribution of Counterions on the Enzyme Surface in Acetonitrile Simulations. In order to determine which regions of the enzyme are more populated by counterions during our simulations, we calculated the probability density maps of the ions during the last 8 ns of simulation. The limited

temporal extent of our acetonitrile simulations (which is a consequence of the poor stability of the enzyme in this media (see the analysis of the Stability of the Simulations, above)) and the low number of ions used could compromise our sampling and bias the distribution of the ions. To avoid this, we used a large number of replicates (20) and tested the convergence of our probability density maps. For each set of simulations, we have divided our sample into two subsets of 10 replicates and calculated the ion probability density maps for each subset. We observed that the maps obtained in the two subsets of simulations are similar (results not shown), which indicates that our sampling is good and that our probability density maps are reliable.

Comparing the maps obtained in the simulations of the X-ray and docked Cl^- ions (Figure 4A and D), we can see that these maps are similar. The similarity between the maps obtained using two distinct methodologies for the initial placement of the ions indicates that the behavior of these ions during the course of the simulations is not strongly biased by the choice of the initial binding sites. Moreover, these results show that the docking methodology that we have been using to place ions in

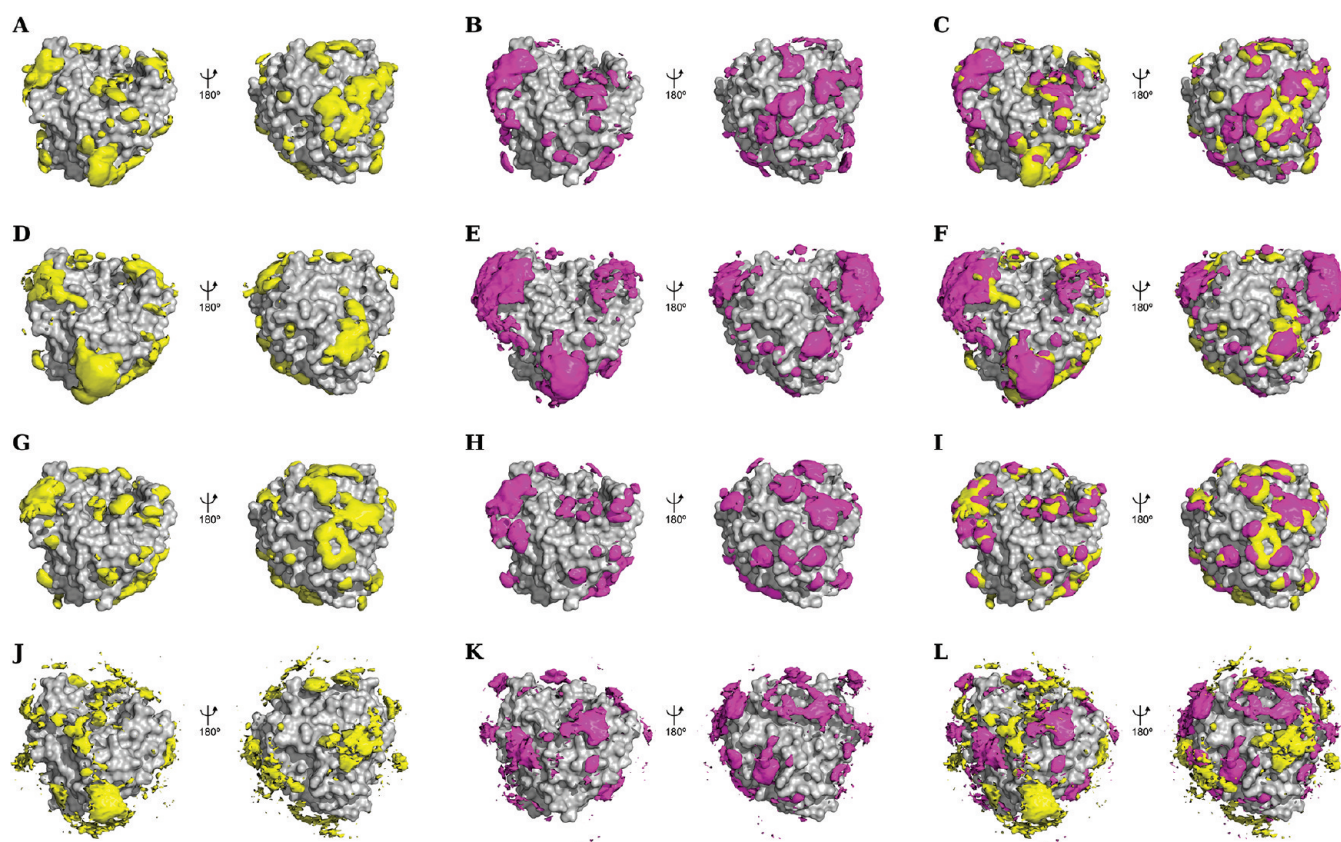


Figure 4. Average probability density maps of chloride (yellow surfaces) and cesium or sodium (magenta surfaces) in the last 8 ns of simulation. The contours enclose regions with a probability density above 2×10^{-5} and $6 \times 10^{-6} \text{ Å}^{-3}$ for acetonitrile and water simulations, respectively. The left-hand column shows the map for Cl^- , the middle column shows the map for Cs^+ or Na^+ , and the right-hand column shows the two maps together. A, B, and C correspond to the simulations with the X-ray ions in acetonitrile. D, E, and F correspond to the simulations with the docked ions in acetonitrile. G, H, and I correspond to the simulations where the X-ray cesium ions were replaced by sodium ions. J, K, and L correspond to the water simulations with 1.5 M CsCl .

our simulations of proteins in nonaqueous media enables a good prediction of Cl^- binding sites.

Comparing the probability density maps of Cs^+ obtained for the simulations with the X-ray and docked ions (Figure 4B and E), we can see that there are overlapping regions, although there are areas that are populated in the simulations performed with the X-ray ions and not in the simulations where ions were placed according to docking predictions. This is probably a consequence of the fact that the number of cesium positions found in the crystal structure is considerably higher than the number of ions found through our docking methodology. However, these cesium positions are not fully occupied in the X-ray structure and would not be expected to be occupied at the same time. Therefore, the probability density maps that were obtained for Cs^+ , in the simulations where the ions were initially placed in the crystallographic positions, are biased by the fact the number of cesium ions used is not realistic (although the sum of the X-ray derived occupancies is reasonable).

As has been mentioned above, one of the aims of this study is to evaluate the consequences of replacing the cesium ions that were found in the X-ray crystal structure by sodium ions. The probability density maps obtained for Cs^+ and Na^+ (Figure 4B and H, respectively) are similar, which means that the two cations populate approximately the same regions of the protein surface. These results support the hypothesis that the Cs^+ binding sites found in the X-ray crystal structure may be

occupied by Na^+ or K^+ in biological conditions, as has been previously proposed,¹ supporting that it is valid to soak crystals with Cs^+ (which is easier to distinguish from water than smaller cations) to identify the positions of Na^+ and K^+ ions. Comparing parts A and G of Figure 4, we can see that the chloride density around the protein surface is considerably lower in the presence of Na^+ than in the presence of Cs^+ , which is a consequence of the tendency of Cl^- to pair with Na^+ and migrate to the bulk solution. Some difference in the behavior of Cs^+ and Na^+ ions is consistent with the difference in catalytic activity between crystals soaked with these different salts.¹

With the purpose of analyzing the behavior of chloride, cesium, and sodium ions during the time course of the simulations, we looked at the evolution of the probability density maps of the ions. In our analysis, we divided the simulations in 10 windows of 1 ns each and calculated the probability density map for each window. All the replicates were included in the calculation, and therefore, the maps represent the average probability density. In jp303008g_si_002.avi (see the Supporting Information), we can see that the crystallographic chloride ions, which are concentrated around their original binding sites in the beginning of the simulations, tend to get more dispersed as the simulation progresses, and occupy a larger portion of the protein surface. The analysis of the trajectories of the MD simulations indicates that most anions explore large regions around the initial position but rarely move to distant areas or

abandon the protein surface. Interestingly, it can be observed that ions that were found in the bottom right area of the protein in the crystal structure migrate slightly down and to the center of the enzyme and end up occupying a region that was found by our docking methodology to have a strong interaction with Cl^- . The docked Cl^- ions are more stable than their X-ray crystal structure counterparts and, in most cases, remain concentrated around their original binding sites throughout the simulations (movie jp303008g_si_005.avi in the Supporting Information). As can be seen in jp303008g_si_003.avi and jp303008g_si_004.avi (available in the Supporting Information), cesium ions are very rapidly dispersed, both in the simulations performed with the X-ray ions and in the ones where the ions were placed according to our docking methodology. It is clear from these movies that these cations are very dynamic. As has been mentioned above, we analyzed the effect of replacing cesium by sodium ions. Looking at jp303008g_si_007.avi (available in the Supporting Information), which shows the behavior of sodium ions, and comparing this movie with jp303008g_si_003.avi (also available in the Supporting Information), showing the behavior of cesium ions, we see that the sodium ions are less mobile than the cesium ions. Comparing the behavior of chloride ions in the presence of cesium (jp303008g_si_002.avi) and sodium (jp303008g_si_006.avi) shows that the chloride ions get more dispersed in the presence of sodium.

To complete our study of the interaction between subtilisin and counterions, we analyzed the ions' tendency to remain close to the protein surface, by measuring the temporal evolution of the distance between the ions and the protein (results not shown). This analysis shows that, as could be inferred from the previous results, in the simulations using CsCl, Cl^- ions tend to be close to the protein surface and almost never go to the bulk of the solution (the percentage of time that the ions spend in the solvent is $\approx 3\%$). Cesium ions, on the other hand, move in and out from the protein surface to the solvent and spend around 40% of the time in solution, showing once again a very dynamic behavior. When the cation used is Na^+ instead of Cs^+ , the situation changes considerably. In these simulations, chloride ions spend a larger percentage of time ($\approx 11\%$) in solution and sodium ions are less frequently found in the solution bulk ($\approx 24\%$ of the total simulation time) than cesium ions. Interestingly, we observed that the Cl^- and Na^+ ions tend to go into the bulk solution as ion pairs and not as isolated ions. The percentage of time that isolated ions pass in solution is around 1% for Cl^- (comparable to the simulations with Cs^+) and 11% for Na^+ ions (considerably lower than the 40% value obtained for Cs^+). In the simulations using Cs^+ ions, we did not observe this behavior and the ions that go into the bulk solution, in the great majority of cases, migrate alone and not as ion pairs.

The higher tendency of cesium and sodium ions to move into the solution bulk when compared with chloride ions can be explained on the basis of the evidence showing that acetonitrile (and polar aprotic solvents in general) solubilize positive ions considerably better than negative ions.^{65–70} This difference is most likely due to the fact that, in aprotic solvents, the negative end of the dipole is concentrated in a small, accessible part of the molecule, whereas the positive end of the dipole is distributed over a large and difficult to access region.^{67,68} Although Na^+ has been shown to have a more negative absolute free energy of solvation in acetonitrile than Cs^+ ,⁷⁰ we observed that cesium ions spend more time in the bulk solution than

sodium ions. This finding can be attributed to the higher tendency of sodium ions to interact with the protein's charged or polar groups and is in line with the results obtained in the PMF analysis which showed that the Na^+Cl^- ion pair was more stable than the Cs^+Cl^- pair. This observation is also consistent with previous studies,^{71–73} where it was found that Na^+ binds more strongly to protein surfaces than K^+ . This finding was attributed to the fact that cations tend to pair with anions of similar surface densities,⁷⁴ and sodium matches carboxylate anions (found in glutamate and aspartate residues) better than potassium. The difference between Na^+ and Cs^+ is expected to be even more pronounced, because cesium has a much lower surface charge density. It is worth noting that the former results were obtained in water, and this is a solvent-dependent effect; i.e., the tendency to form an ion pair depends on a delicate balance between the cost of desolvating the ions and the benefit of forming the ion pair. Given that the differences between the solvation free energies of Na^+ and Cs^+ in water and acetonitrile are similar,⁷⁰ the same trend should be observed in the two solvents, which is in agreement with our results.

Distribution of Counterions on the Enzyme Surface in Water Simulations.

In order to analyze how counterions interact with subtilisin in water, we have performed MD simulations in which the enzyme was placed in an aqueous solution containing 1.5 M CsCl. In the beginning of these simulations, the ions were randomly distributed in the most external region of the water box, far from the protein. Not surprisingly, the ions do not form very stable interactions with the enzyme and spend 98.2% (for Cl^-) and 95.5% (for Cs^+) of the time in solution. Nevertheless, there are some regions of the protein surface where the ions accumulate. Looking at Figure 4, we can see that, although there are clear differences between the maps obtained in water (Figure 4J and L) and acetonitrile (Figure 4A and C), there is some overlap between them. This indicates that, although the nature of the solvent influences the interaction between counterions and the protein, some binding sites are conserved in different solvents. Additionally, Figure 4C and L shows that Cl^- and Cs^+ ions tend to be close to each other in acetonitrile (the yellow and magenta surfaces often overlap) but not in water.

The crystallographic structure of subtilisin, crystallized in aqueous conditions and soaked with a solution containing 1.5 M CsCl (Cianci et al. (to be published)), has recently been determined at 2.28 Å resolution. This structure enabled the identification of a significant number of ion binding sites in this aqueous crystal environment, which were compared with the distributions of the ions in the MD simulations in water. Figure 5 shows the probability density maps obtained in the aqueous simulations with 1.5 M CsCl and the positions of the ions in the X-ray structure obtained in aqueous conditions (Cianci et al. (to be published)). In Figure 5A, we can see that there is almost no overlap between the map obtained for Cl^- and the positions that were found in the X-ray structure. The distribution of cesium ions in our simulations shows some agreement with the binding sites found in the X-ray structure (Figure 5B). Examining the locations of chloride and cesium ions in the crystal structure, we observed that two chloride and two cesium ions are interacting with more than one molecule in the crystal. These crystal contacts can create artificial binding sites that will not be found in solution, and this can explain why the ions did not populate these sites in our simulations. However, for the binding sites which are not formed by more than one enzyme molecule, there has to be an alternative

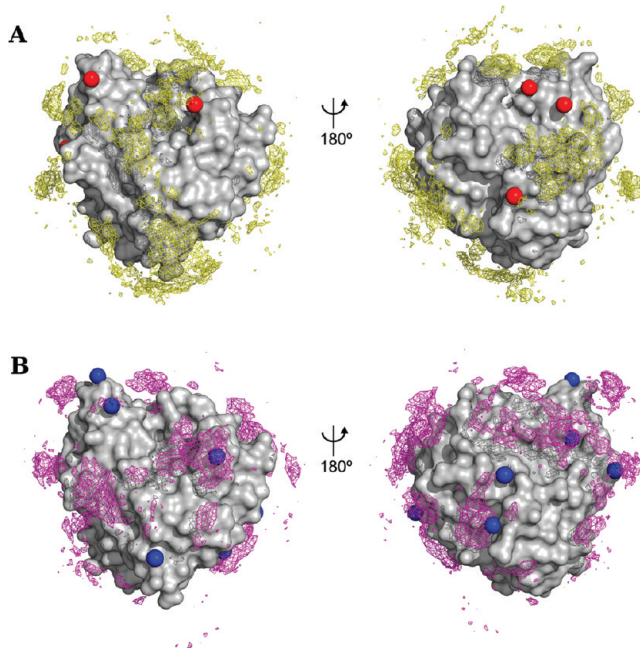


Figure 5. Comparison of the probability density maps (represented using a mesh) for chloride (A) and cesium ions (B) obtained in the MD simulations in water using 1.5 M CsCl with the positions of the chloride (red spheres) and cesium (blue spheres) ions in the crystal structure obtained in aqueous conditions (Cianci et al. (to be published)). The contours enclose regions with a probability density above $6 \times 10^{-6} \text{ Å}^{-3}$.

explanation for the disagreement between the X-ray and MD simulation results. In an attempt to understand these differences, we calculated the electrostatic potential in the crystal and in solution. This calculation was done using the *potential* tool, available in the Mead package,⁷⁵ version 2.2.5, and assigning dielectric constants of 2.0 and 80.0 to the protein interior and solvent, respectively. To simulate the crystal environment, we reconstructed the neighboring asymmetric units from the PDB file using the software PyMOL⁷⁶ (www.pymol.org). All water molecules and chloride and cesium ions were removed from the structure, in order to investigate the

potential created by the protein alone. Our calculations indicate that the crystal environment strongly influences the electrostatic potential on the protein surface (see Figure S7 in the Supporting Information). In the crystal, a large fraction of the protein surface has a positive potential, whereas in solution this is not observed. Looking at the potential in the chloride X-ray binding sites, we observed that in most cases it is clearly positive in the crystal environment and becomes more negative in solution. This explains why the chloride binding sites found in the X-ray structure are not very populated during the simulations. In what concerns the potential in the cesium binding sites, we observed that, in general, it is more negative in solution than in the crystal and, therefore, in this case we have a better agreement between the theoretical and experimental results.

Analyzing the Effect of Different Cations on the Activity of Subtilisin. In a previous work, it was observed that the type of counterion used influences the catalytic activity of subtilisin crystals in acetonitrile: using a larger cation gives a larger rate enhancement.¹ In order to rationalize this observation, we decided to compare the distribution of counterions in the active site of subtilisin, in the simulations using CsCl and NaCl. As was mentioned above, our pK_a calculations indicate that, at a pH of 6.5, the catalytic histidine can be either fully protonated or have only one proton (with probabilities of ≈ 70 and $\approx 30\%$, respectively). Therefore, for each salt used, we have performed MD simulations considering the two possible protonation states of H64 and analyzed how the ions are distributed around the active site of subtilisin in the four sets of simulations. In Figure 6, we can observe that, in the simulations where H64 is protonated and therefore positively charged, there is an accumulation of chloride ions very close to this residue when the cation used is Cs^+ (Figure 6A). This is not observed when the histidine is neutral (Figure 6B). Curiously, when the cation used is Na^+ , we do not observe such a high concentration of chloride in the vicinity of the catalytic histidine (Figure 6C). The radial distribution functions displayed in Figure S8 (see the Supporting Information) show that Cl^- has a considerably higher probability of forming an ionic interaction with H64 when the cation used is Cs^+ compared with Na^+ , which is probably a consequence of the

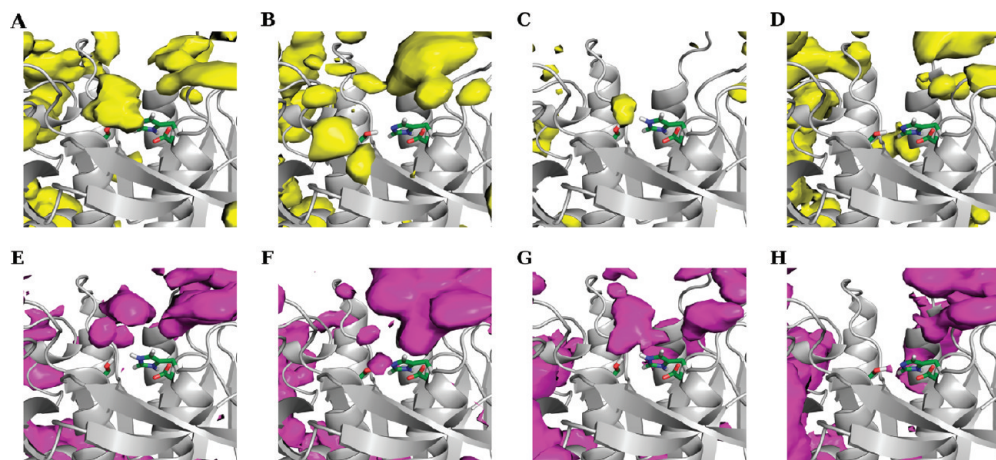


Figure 6. Probability density maps of chloride (yellow surfaces) and cesium or sodium (magenta surfaces) ions in the active site of subtilisin in acetonitrile simulations. The contours enclose regions with a probability density above $2 \times 10^{-5} \text{ Å}^{-3}$. A and E correspond to the simulations with CsCl and charged H64; B and F correspond to the simulations with CsCl and neutral H64; C and G correspond to the simulations with NaCl and charged H64; D and H correspond to the simulations with NaCl and neutral H64.

higher tendency of Cl^- to bind to Na^+ than to Cs^+ . From these results, one would expect that in the presence of Cs^+ the charged state of H64 would be more stabilized (due to the higher concentration of Cl^- in the vicinity of H64) than in the presence of Na^+ . Therefore, one would predict that subtilisin would be more active when Na^+ is used instead of Cs^+ , because it is accepted that the catalytic histidine needs to be in the neutral state in order to be active. However, this is inconsistent with the experimental observations, which indicate that subtilisin is more active in the presence of larger cations. In the light of these observations, we propose an alternative explanation, which is to consider that the Cl^- ion could accept the proton from H64, stabilizing the catalytically active neutral state. Although this may seem counterintuitive because we are used to thinking in aqueous conditions, it is possible that in a moderately polar medium like acetonitrile the equilibrium represented in eq 1 is shifted toward the right side. A good indication that this hypothesis is plausible is the fact that a value of 10.3 has been determined for the pK_a of HCl in acetonitrile.⁷⁷



Given that there are more chloride ions available when the cation used is Cs^+ than when Na^+ is used (because the Na^+Cl^- is more stable than the Cs^+Cl^- pair), the neutral state of H64 would be more stabilized in the presence of Cs^+ and this would explain why subtilisin is more active in the presence of CsCl.

We emphasize that the proposed explanation described above is just one hypothesis. We do not have enough evidence to confirm it, and we do not exclude that other factors might contribute to the cation dependence of subtilisin activity. However, we think our explanation is plausible, and it opens the door for future studies, which may clarify this question.

CONCLUSIONS

In this work, we used molecular dynamic simulations to complement the X-ray crystallographic analysis of the interaction between subtilisin and counterions in acetonitrile, performed in a previous work.¹ In order to analyze the interaction between subtilisin and counterions in acetonitrile and to characterize the dynamic behavior of the system, we performed two different sets of simulations in acetonitrile. In the first set, the initial positions of cesium and chloride ions were the ones available in the X-ray crystal structure determined after soaking with CsCl. In the second set, we used a methodology based on docking simulations to find the ion binding sites, and then started the MD simulations with the ions placed in those locations. Our results indicate that some of the chloride binding sites found in the X-ray crystal structure are highly populated during the simulations, whereas others are rarely occupied. The Cl^- binding sites determined using the docking methodology have high occupancies in the MD simulations. Cesium binding sites have low occupancies independently of the method that was used to define their initial binding sites. We also observed that chloride ions tend to stay close to the protein, whereas cesium ions are considerably more dynamic and frequently move into the bulk solution. Comparing the distribution of the ions in the two sets of simulations, we observed that they are reasonably similar, which indicates that the simulations are not strongly biased by the initial locations of the ions.

Additionally, we performed simulations in which the crystallographic cesium ions were replaced by sodium ions.

The distribution of sodium and cesium ions around the protein surface is similar, indicating that the Cs^+ binding sites found in the X-ray crystal structure may be occupied by Na^+ or K^+ in biological conditions, as previously proposed.¹ Therefore, using soaking with Cs^+ as a method to identify the position of Na^+ and K^+ is here validated. We also observed that Cl^- and Na^+ ions frequently form ion pairs and move into the bulk solution together. This leads to a decrease in the concentration of chloride ions bound to the protein. Most interestingly, this is observed in the vicinity of the catalytic histidine, when this residue is positively charged. We propose that, in acetonitrile, chloride can accept the proton from the charged H64, moving the equilibrium toward the catalytically active neutral state, which can explain the previous experimental observations showing that subtilisin is more active when the cation present is Cs^+ or choline when compared with smaller cations.¹

In addition to the acetonitrile simulations, we performed simulations in water, using 1.5 M CsCl. The analysis of the probability density maps showed that there are some differences in the distribution of the ions around the enzyme surface in water and acetonitrile, although the maps have some overlapping regions. Additionally, we observed that in water the ions are much more frequently found in the bulk solution than in acetonitrile. These results indicate that the solvent influences the interaction between the ions and the protein. Comparing the probability density maps obtained in our simulations with the positions of the ions in the X-ray crystal structure obtained in an aqueous medium (Cianci et al. (to be published)), we observed that there is some agreement in the case of cesium but not in the case of chloride ions. The difference between the results obtained in the simulations and the chloride binding sites found in the crystal structure can be explained by the fact that the crystal lattice can generate an electrostatic potential which is very different from the one found in solution.

ASSOCIATED CONTENT

Supporting Information

Protocol for selecting counterion positions using molecular docking. Methodology used to randomly distribute Cs^+ and Cl^- ions in the simulations performed in water. Protocol for modeling protein protonation equilibrium. Description of the systems' preparation for MD simulations. Analysis of the potentials of mean force. Protonation of ionizable residues at pH 6.5. Electrostatic surface maps of subtilisin in the crystal environment and in solution. Radial distribution function of Cl^- around the Ne_2 of H64. Six movies showing the temporal evolution of the probability density maps of the ions in the simulations performed. This material is available free of charge via the Internet at <http://pubs.acs.org>.

AUTHOR INFORMATION

Corresponding Author

*Mailing address: Protein Modelling Laboratory, ITQB-UNL, Av. da República, 2780-157 Oeiras, Portugal. Phone: +351214469610. Fax: +351214411277. E-mail: claudio@itqb.unl.pt.

Notes

The authors declare no competing financial interest.

ACKNOWLEDGMENTS

The authors acknowledge Dr. Nuno Micaêlo, Dr. Susana Barreiros, and Dr. André Melo for helpful discussions and the

financial support from Fundação para a Ciência e a Tecnologia, Portugal, through grants SFRH/BD/28269/2006, POCTI/BIO/57193/2004, and PEst-OE/EQB/LA0004/2011. M.C., P.J.H., and J.R.H. are grateful to the Synchrotron Radiation Source at STFC Daresbury Laboratory for X-ray beamtime; details are as described in ref 1. The EMBL Hamburg (M.C.), the University of Manchester (J.R.H.), and Strathclyde University (P.J.H.) are thanked for general support; details are again as described in ref 1.

■ REFERENCES

- (1) Cianci, M.; Tomaszewski, B.; Helliwell, J. R.; Halling, P. J. *J. Am. Chem. Soc.* **2010**, *132*, 2293.
- (2) Klibanov, A. M. *Nature* **2001**, *409*, 241.
- (3) Deshpande, A.; Nimsadkar, S.; Mande, S. C. *Acta Crystallogr., Sect. D Biol. Crystallogr.* **2005**, *61*, 1005.
- (4) English, A. C.; Done, S. H.; Caves, L. S. D.; Groom, C. R.; Hubbard, R. E. *Proteins: Struct., Funct., Genet.* **1999**, *37*, 628.
- (5) Gao, X. G.; Maldonado, E.; Perez-Montfort, R.; Garza-Ramos, G.; De Gomez-Puyou, M. T.; Gomes-Puyou, A.; Rodriguez-Romero, A. *Proc. Natl. Acad. Sci. U.S.A.* **1999**, *96*, 10062.
- (6) Mattos, C.; Bellamacina, C. R.; Peisach, E.; Pereira, A.; Vitkup, D.; Petsko, G. A.; Ringe, D. *J. Mol. Biol.* **2006**, *357*, 1471.
- (7) Schmitke, J. L.; Stern, L. J.; Klibanov, A. M. *Proc. Natl. Acad. Sci. U.S.A.* **1998**, *95*, 12918.
- (8) Zhu, G. Y.; Huang, Q. C.; Wang, Z. M.; Qian, M. X.; Jia, Y. S.; Tang, Y. Q. *Biochim. Biophys. Acta* **1998**, *1429*, 142.
- (9) Zhu, G. Y.; Huang, Q. C.; Zhu, Y. S.; Li, Y. L.; Chi, C. W.; Tang, Y. Q. *Biochim. Biophys. Acta, Protein Struct. Mol. Enzymol.* **2001**, *1546*, 98.
- (10) Soares, C. M.; Teixeira, V. H.; Baptista, A. M. *Biophys. J.* **2003**, *84*, 1628.
- (11) Cruz, A.; Ramirez, E.; Santana, A.; Barletta, G.; Lopez, G. E. *Mol. Simul.* **2009**, *35*, 205.
- (12) Hartsough, D. S.; Merz, K. M. *J. Am. Chem. Soc.* **1993**, *115*, 6529.
- (13) Hartsough, D. S.; Merz, K. M. *J. Am. Chem. Soc.* **1992**, *114*, 10113.
- (14) Toba, S.; Hartsough, D. S.; Merz, K. M. *J. Am. Chem. Soc.* **1996**, *118*, 6490.
- (15) Micaelo, N. M.; Soares, C. M. *J. Phys. Chem. B* **2008**, *112*, 2566.
- (16) Micaelo, N. M.; Soares, C. M. *FEBS J.* **2007**, *274*, 2424.
- (17) Micaelo, N. M.; Teixeira, V. H.; Baptista, A. M.; Soares, C. M. *Biophys. J.* **2005**, *89*, 999.
- (18) Zaks, A.; Klibanov, A. M. *J. Biol. Inorg. Chem.* **1988**, *263*, 8017.
- (19) Bell, G.; Halling, P. J.; Moore, B. D.; Partridge, J.; Rees, D. G. *Trends Biotechnol.* **1995**, *13*, 468.
- (20) Bell, G.; Janssen, A. E. M.; Halling, P. J. *Enzyme Microb. Technol.* **1997**, *20*, 471.
- (21) Halling, P. J. *Biochim. Biophys. Acta* **1990**, *1040*, 225.
- (22) Halling, P. J. *Philos. Trans. R. Soc. London, Ser. B* **2004**, *359*, 1287.
- (23) Colombo, G.; Toba, S.; Merz, K. M. *J. Am. Chem. Soc.* **1999**, *121*, 3486.
- (24) Ke, T.; Klibanov, A. M. *J. Am. Chem. Soc.* **1998**, *120*, 4259.
- (25) Ke, T.; Tidor, B.; Klibanov, A. M. *Biotechnol. Bioeng.* **1998**, *57*, 741.
- (26) Ke, T.; Wescott, C. R.; Klibanov, A. M. *J. Am. Chem. Soc.* **1996**, *118*, 3366.
- (27) Ke, T.; Klibanov, A. M. *Biotechnol. Bioeng.* **1998**, *57*, 746.
- (28) Klibanov, A. M. *Nature* **1995**, *374*, 596.
- (29) Lousa, D.; Baptista, A. M.; Soares, C. M. *Protein Sci.* **2011**, *20*, 379.
- (30) Russell, A. J.; Klibanov, A. M. *J. Biol. Chem.* **1988**, *263*, 11624.
- (31) Staahl, M.; Jeppsson-Wistrand, U.; Maansson, M. O.; Mosbach, K. *J. Am. Chem. Soc.* **1991**, *113*, 9366.
- (32) Serdakowski, A. L.; Dordick, J. S. *Trends Biotechnol.* **2008**, *26*, 48.
- (33) Der, A. *Biotechnol. Biotechnol. Equip.* **2008**, *22*, 629.
- (34) Yu, H. W.; Chen, H.; Yang, Y. Y.; Ching, C. B. *J. Mol. Catal. B* **2005**, *35*, 28.
- (35) Zhao, H. *J. Mol. Catal. B* **2005**, *37*, 16.
- (36) Ru, M. T.; Hirokane, S. Y.; Lo, A. S.; Dordick, J. S.; Reimer, J. A.; Clark, D. S. *J. Am. Chem. Soc.* **2000**, *122*, 1565.
- (37) Morgan, J. A.; Clark, D. S. *Biotechnol. Bioeng.* **2004**, *85*, 456.
- (38) Altreuter, D. H.; Dordick, J. S.; Clark, D. S. *J. Am. Chem. Soc.* **2002**, *124*, 1871.
- (39) Bilanicova, D.; Salis, A.; Ninham, B. W.; Monduzzi, M. *J. Phys. Chem. B* **2008**, *112*, 12066.
- (40) Lindsay, J. P.; Clark, D. S.; Dordick, J. S. *Biotechnol. Bioeng.* **2004**, *85*, 553.
- (41) Eppler, R. K.; Komor, R. S.; Huynh, J.; Dordick, J. S.; Reimer, J. A.; Clark, D. S. *Proc. Natl. Acad. Sci. U.S.A.* **2006**, *103*, 5706.
- (42) Halling, P. J. *Curr. Opin. Chem. Biol.* **2000**, *4*, 74.
- (43) Schmitke, J. L.; Stern, L. J.; Klibanov, A. M. *Proc. Natl. Acad. Sci. U.S.A.* **1997**, *94*, 4250.
- (44) Fitzpatrick, P. A.; Ringe, D.; Klibanov, A. M. *Biochem. Biophys. Res. Commun.* **1994**, *198*, 675.
- (45) Fitzpatrick, P. A.; Steinmetz, A. C. U.; Ringe, D.; Klibanov, A. M. *Proc. Natl. Acad. Sci. U.S.A.* **1993**, *90*, 8653.
- (46) Hess, B.; Holm, C.; van der Vegt, N. *Phys. Rev. Lett.* **2006**, *96*, 164509.
- (47) Hess, B.; Holm, C.; van der Vegt, N. *J. Chem. Phys.* **2006**, *124*, 147801.
- (48) Hess, B.; Bekker, H.; Berendsen, H. J. C.; Fraaije, J. G. E. M. *J. Comput. Chem.* **1997**, *18*, 1463.
- (49) Baptista, A. M.; Martel, P. J.; Soares, C. M. *Biophys. J.* **1999**, *76*, 2978.
- (50) Baptista, A. M.; Soares, C. M. *J. Phys. Chem. B* **2001**, *105*, 293.
- (51) Berendsen, H. J. C.; van der Spoel, D.; van Drunen, R. *Comput. Phys. Commun.* **1995**, *91*, 43.
- (52) Hess, B.; Kutzner, C.; van der Spoel, D.; Lindahl, E. *J. Chem. Theory Comput.* **2008**, *4*, 435.
- (53) Oostenbrink, C.; Villa, A.; Mark, A. E.; Van Gunsteren, W. F. *J. Comput. Chem.* **2004**, *25*, 1656.
- (54) Hermans, J.; Berendsen, H. J. C.; van Gunsteren, W. F.; Postma, J. P. M. *Biopolymers* **1984**, *23*, 1513.
- (55) Gee, P. J.; Van Gunsteren, W. F. *Mol. Phys.* **2006**, *104*, 477.
- (56) Reif, M. M.; Hunenberger, P. H. *J. Chem. Phys.* **2011**, *134*, 144104.
- (57) Miyamoto, S.; Kollman, P. A. *J. Comput. Chem.* **1992**, *13*, 952.
- (58) Berendsen, H. J. C.; Postma, J. P. M.; van Gunsteren, W. F.; Dinola, A.; Haak, J. R. *J. Chem. Phys.* **1984**, *81*, 3684.
- (59) van Gunsteren, W. F.; Berendsen, H. J. C. *Angew. Chem., Int. Ed.* **1990**, *29*, 992.
- (60) Barker, J. A.; Watts, R. O. *Mol. Phys.* **1973**, *26*, 789.
- (61) Tironi, I. G.; Sperb, R.; Smith, P. E.; van Gunsteren, W. F. *J. Chem. Phys.* **1995**, *102*, 5451.
- (62) Smith, P. E.; Pettitt, B. M. *J. Phys. Chem.* **1994**, *98*, 9700.
- (63) Barthel, J.; Kleebauer, M.; Buchner, R. *J. Solution Chem.* **1995**, *24*, 1.
- (64) Kabsch, W.; Sander, C. *Biopolymers* **1983**, *22*, 2577.
- (65) Coetze, J. F.; Campion, J. J. *J. Am. Chem. Soc.* **1967**, *89*, 2517.
- (66) Coetze, J. F.; Campion, J. J. *J. Am. Chem. Soc.* **1967**, *89*, 2513.
- (67) Davidson, W. R.; Kebarle, P. *J. Am. Chem. Soc.* **1976**, *98*, 6125.
- (68) Yamdagni, R.; Kebarle, P. *J. Am. Chem. Soc.* **1972**, *94*, 2940.
- (69) Marcus, Y. *Pure Appl. Chem.* **1983**, *55*, 977.
- (70) Kelly, C. P.; Cramer, C. J.; Truhlar, D. G. *J. Phys. Chem. B* **2007**, *111*, 408.
- (71) Vrbka, L.; Vondrasek, J.; Jagoda-Cwiklik, B.; Vácha, R.; Jungwirth, P. *Proc. Natl. Acad. Sci. U.S.A.* **2006**, *103*, 15440.
- (72) Uejio, J. S.; Schwartz, C. P.; Duffin, A. M.; Drisdell, W. S.; Cohen, R. C.; Saykally, R. J. *Proc. Natl. Acad. Sci. U.S.A.* **2008**, *105*, 6809.
- (73) Aziz, E. F.; Ottosson, N.; Eisebitt, S.; Eberhardt, W.; Jagoda-Cwiklik, B.; Vácha, R.; Jungwirth, P.; Winter, B. *J. Phys. Chem. B* **2008**, *112*, 12567.

- (74) Collins, K. D. *Biophys. J.* **1997**, *72*, 65.
- (75) Bashford, D. An object-oriented programming suite for electrostatic effects in biological molecules. In *Scientific Computing in Object-Oriented Parallel Environments*; Ishikawa, Y., Oldhoeft, R. R., Reynders, J. V. W., Tholburn, M., Eds.; Springer: Berlin, 1997; Vol. 1343, p 233.
- (76) DeLano, W. L. *The PyMOL Molecular Graphics System*; DeLano Scientific: Palo Alto, CA: 2003.
- (77) Kutt, A.; Rodima, T.; Saame, J.; Raamat, E.; Maemets, V.; Kaljurand, I.; Koppel, I. A.; Garlyauskayte, R. Y.; Yagupolskii, Y. L.; Yagupolskii, L. M.; Bernhardt, E.; Willner, H.; Leito, I. *J. Org. Chem.* **2011**, *76*, 391.